Available online at www.sciencedirect.com
SCIENCE DIRECT®
Biochemical and Biophysical Research Communications 311 (2003) 139–148
BBRC
www.elsevier.com/locate/ybbrc

Molecular cloning and functional expression of nucleolar phospholipid hydroperoxide glutathione peroxidase in mammalian cells

Toshiyuki Nakamura, Hirotaka Imai, Naomi Tsunashima, and Yasuhito Nakagawa*

School of Pharmaceutical Sciences, Kitasato University, 5-9-1 Shirokane, Minato-ku, Tokyo 108-8641, Japan

Received 25 September 2003

Abstract

We cloned a full-length cDNA for phospholipid hydroperoxide glutathione peroxidase (PHGPx) including exon Ib from rat and mouse testis. The nuclear signal sequence of the N terminal of rat nuclear PHGPx possessed a different sequence from that previously reported for rat sperm nuclei GPx (SnGPx). Expression of this PHGPx–YFP (yellow fluorescent protein) fusion protein including a novel nuclear signal sequence was exclusively localized in nucleolus; although YFPs fused with only a novel nuclear signal sequence were distributed in the whole nucleus, indicating that preferential translocation of nucleolar PHGPx into nucleoli was required for the nuclear signal sequence and internal sequence of PHGPx. Low level expression of nucleolar PHGPx was detected in several tissues, but the expression of nucleolar PHGPx was extensively high in testis. Immunohistochemical analysis with anti-nucleolar PHGPx indicated that expression of nucleolar PHGPx was observed in the nucleoli in the spermatogonia, spermatocyte, and spermatid. Overexpression of 34 kDa nucleolar PHGPx in RBL2H3 cells significantly suppressed cell death induced by actinomycin D and doxorubicin that induced damage in the nucleolus. These results indicated that nucleolar PHGPx plays an important role in prevention of nucleolus from damage in mammalian cells.

Keywords: PHGPx; Nucleolus; Nuclear targeting signal; Overexpression; Cell death

Phospholipid hydroperoxide glutathione peroxidase (PHGPx) is a unique intracellular antioxidant enzyme that directly reduces peroxidized phospholipids that have been produced in cell membranes [1]. From cloning of PHGPx genomic DNA, there are seven exons encoding mitochondrial and non-mitochondrial PHGPx [2–4]. The mitochondrial targeting signal of PHGPx and the initial start codon of non-mitochondrial PHGPx are in first exon Ia of PHGPx genomic DNA. Recently, Pfeifer et al. found a 34 kDa sperm nuclei specific selenoprotein (SnGPx), in which the N-terminal amino acid sequence was identified as a different first exon Ib that exists between exon Ia and exon II in the genomic DNA [5]. 34 kDa SnGPx is highly expressed in the nuclei of late spermatids and spermatozoa [5,6]. We recently indicated that the expression levels of 34 kDa SnGPx, and mitochondrial and non-mitochondrial PHGPx decreased to a half in testis of PHGPx heterozygous mice compared to wild types by the disruption of all PHGPx exons including exon Ia and exon Ib, so that PHGPx gene knockout mice became embryonic lethal [2]. These results indicate that three types of PHGPx, mitochondrial, non-mitochondrial PHGPx, and SnGPx, are transcribed from one gene by alternative transcription and that all are important for normal mouse development. Exon Ib includes a nuclear targeting signal because fluorescence of GFP with only exon Ib for rat SnGPx was distributed within the nucleus [5]. This nuclear type of PHGPx is thought to play an important role in the stabilization of condensed chromatin and in the protection of sperm DNA from oxidation in spermatogenesis [5,6]. However, details of the tissue distribution of this nuclear type of PHGPx and its function in mammalian cells are unclear. On the other hand, recently our studies using mitochondrial and non-mitochondrial PHGPx overexpressing RBL2H3 cells have

* Corresponding author. Fax: +81-3-5791-6236.
E-mail address: nakagaway@pharm.kitasato-u.ac.jp (Y. Nakagawa).

0006-291X/$ - see front matter © 2003 Elsevier Inc. All rights reserved.
doi:10.1016/j.bbrc.2003.09.183

shown that the mitochondrial and non-mitochondrial PHGPx play several important but independent roles in the modulation of signal transduction, inflammation, spermatogenesis, and apoptosis [7–16]. Thus overexpression of different types of PHGPx in a RBL2H3 cell line has provided a useful model system to clarify the cellular functions of different types of PHGPx. However, there are no reports of the expression of, or a functional analysis of, full-length cDNA for snGPx, a nuclear type of PHGPx, in mammalian cells.

We show that this nuclear type of PHGPx is selectively localized in nucleolus in mammalian cells, and that targeting of nucleolar PHGPx into nucleoli is required for the nuclear signal sequence in the N terminus and the internal amino acid sequence of PHGPx. We name it as nucleolar PHGPx and to clarify its cellular function we establish nucleolar PHGPx overexpressing cells for the first time. The overexpression of nucleolar PHGPx suppresses cell death by actinomycin D and doxorubicin that induce damage in the nucleolus.

Materials and methods

Detection and molecular cloning of nucleolar PHGPx cDNA. We previously cloned and sequenced PHGPx genomic DNA from a mouse 129/SV genomic library (Accession No. AB030643; [2]). We designed the primers on the basis of the sequence of the mouse genomic exon Ib and exon VII as shown in Fig. 1A. The cDNA was synthesized from total RNA extracted from testis of Balb/c mouse and Sprague–Dawley rat using M-MLV reverse transcriptase (Bibco BRL) with random primer (TAKARA Shuzo). The PCRs were performed from the cDNAs by LA*Taq* DNA polymerase (TAKARA Shuzo) with two primers as follows; primers NF1, 5′-ATTGGATCCAGACCGGCG GGCATGGGCCGCGCG-3′ and NR1, 5′-ATTGGATCCTTCTAC ATTTTATTCCCAC-3′. The resulting products of PCR for mouse and rat were subcloned into the *Bam*HI site of plasmid pTZ18R to yield plasmid pMNPHGPx1 and pRNPHGPx1. The nucleotide sequence was determined from both strands of DNA with an Autocycle Sequencing Kit and a model LKB ALF red DNA sequencer (Pharmacia). 5′-rapid amplification of the cDNA end (5′-RACE) was carried out with the 5′-Full RACE Core Set (Takara Shuzo) according to the manufacturer's instructions. cDNA was synthesized from total RNA extracted from Balb/c mouse and SD rat testis using AMV reverse transcriptase XL and a 5′-end phosphorylated RR1 primer, 5′- CAA GCCCAGGAACTCGTGGCTG-3′ for rat and MR1 primer, 5′-CA AGCCCAGGAACTCGGAGCTG-3′ for mouse at 50 °C for 60 min. The cDNA was ligated and concentrated using T4 RNA ligase (Takara Syuzo). PCR was performed with LA*Taq* DNA polymerase (TAKA RA Shuzo) using first PCR primer sets, RS2, 5′-CAGGCCCTCGGA GGAGGAGAGCTCGCG-3′ for rat, MS2, 5′-CGGGCCCTCGGCG AAGGAAAGCGCGCG-3′ for mouse and RR2, 5′-GGACTTTGG CGTCCAGGTTCACGCCGT-3′ for rat, MR2, 5′-GGACTTTGGC GTCCAGGTCCACGGCGT-3′ for mouse and nested PCR primer sets and RS3, 5′-AACCCGCGGCCTCTGCTGCAGGACCTT-3′ for rat, MS3, 5′-AACCCGGGGCCTCTGCTGCAAGAGCCT-3′ for mouse and RR3, 5′-GCCGCGCTGTCTGCAGCGTCCCCGCTT-3′ for both rat and mouse. The 5′-RACE-generated fragments were cloned into a pT7 Blue Blunt Vector (Novagen) and completely sequenced in the directions of sense and antisense strands with a model LKB ALF red DNA sequencer (Pharmacia). For detection of nucleolar PHGPx mRNA in various tissues, first PCR was performed from cDNA synthesized from total RNA of various tissues by M-MLV reverse transcriptase using LA*Taq* DNA polymerase with the primer sets, NF1 and NR1, described above. The bands around 985 bp amplified by the first PCR were extracted from 1% agarose gel and the second PCR and nested PCR were performed from a thousand dilution of the product of the first PCR using LA*Taq* DNA polymerase with the first PCR primer sets, NF1, NR1, and nested PCR primer sets, RS3 and NR2; 5′-GCCGCGCTGTCTGCAGCGTCCCCGCTT-3′.

Cell culture. Human HeLa cells, mouse L929 cells, rat RBL2H3 cells, and S1 cells that were transfected with pSRα and pSV2neo as described previously [8] were cultured in Dulbecco's modified essential medium (DMEM) that contained 2 mM glutamine, penicillin (100 U/ml), streptomycin (100 U/ml), and 5% fetal calf serum (FCS).

Construction and visualization of three types of PHGPx–YFP fusion protein. To study the subcellular localization of three types of PHGPx, three recombinant plasmids, named nucleolar PHGPx–YFP (yellow fluorescent protein), mitochondrial PHGPx–YFP, non-mitochondrial PHGPx–YFP, and Ib–YFP were constructed as follows; the cDNA clones (pRPHGPx5) encoding the mitochondrial PHGPx (Cys) we constructed previously [3] contained that first initiation codon including exon Ia and mutation that converted UGA, which encodes selenocysteine, to UGU, which encodes cysteine. To construct the rat nucleolar PHGPx (Cys) containing a novel nuclear signal peptide, the clone pRNPHGPx2 was constructed by insertion of the *Bam*HI–*Cla*I fragment of pRNPHGPx1 between the *Bam*HI and *Cla*I sites of pRPHGPx5. To construct three types of PHGPx–YFP fusion proteins, the sequences corresponding to the predicted three types of PHGPx were amplified by PCR from pRNPHGPx2 for nucleolar PHGPx, and pRPHGPx5 for mitochondrial PHGPx and non-mitochondrial PHGPx using the sense primers, NuPS, 5′-ATTGGATCCGGCCG CCGAGA TGGGCCGCGCGGCCGCCCGCAA-3′ for nucleolar PHGPx, MTPS, 5′-ATTGGATCCGGCCGCCGAGATGAGCTGG GGCCGTCT-3′ for mitochondrial PHGPx, and CPS, 5′-ATTGGAT CCGGCTGGCACCATGTGTGCA-3′ for non-mitochondrial PHGPx, and common antisense primers, FAS, 5′-ATTGGATCCGCGAGAT AGCACGGCAGGTC-3′. The PCR-amplified fragments were digested with *Bam*HI and cloned in-frame into the *Bam*HI sites of the pEYFP-N1 vector (Clontech). To construct the Ib–YFP fusion protein, exon Ib was amplified by PCR from pRNPHGPx2 using sense primer, IbS; 5′-ATTAAGCTTGGCCGCCGAGATGGGCCGCGC GGCCGCCCGCAA-3′ and antisense primer, IbAS; 5′-AATTGG GATCCAAGCCCAGGAACTCGTGG-3′. The PCR fragment was inserted between the *Hin*dIII and *Bam*HI sites of the pEYFP-N1 and its sequence was checked before proceeding. For expression and visualizing, HeLa cells and RBL2H3 cells were seeded at 1×10^5 cells on 14-mm cover glass 1 day before transfection. The cells were transfected with 500 ng each of PHGPx–YFP fusion vector using 50 μl lipofectamine plus reagents and 2 μl lipofectamine reagent for 6 h (Invitrogen) as described in the manufacturer's recommendation. After 6 h cell culture, cells were fixed for 5 min on cover glass with 10% formaldehyde and washed with phosphate buffered saline (PBS). Cells were stained with 1.6 μM Hoechst 33258 for 5 min. After three washes with PBS, the samples were treated with Aqua-Poly/Mount (Polysciences, Warrington, PA) before mounting. Samples were analyzed using a confocal microscope LSM510 META (Carl Zeiss). The nucleolar localization of nucleolar PHGPx–YFP fusion protein was confirmed by immunostaining with Cy3 conjugated anti-nucleolar specific protein C23 mAb (Santa Cruz) according to methods described previously [9].

Preparation of antibodies against 34 kDa nucleolar PHGPx and immunohistochemisty. Undecapeptide [GRAAARKRGRC] corresponding to amino terminal sequence of rat and mouse 34 kDa nucleolar PHGPx was conjugated to keyhole limpet hemocyanin with a linkage between cysteine at the carboxyl terminal of the peptides and a bifunctional spacer. The conjugates were used to immunize rabbit by subcutaneous injection. After two booster injections at 2-week intervals, anti-34 kDa nucleolar PHGPx polyclonal antibodies (pAb) were

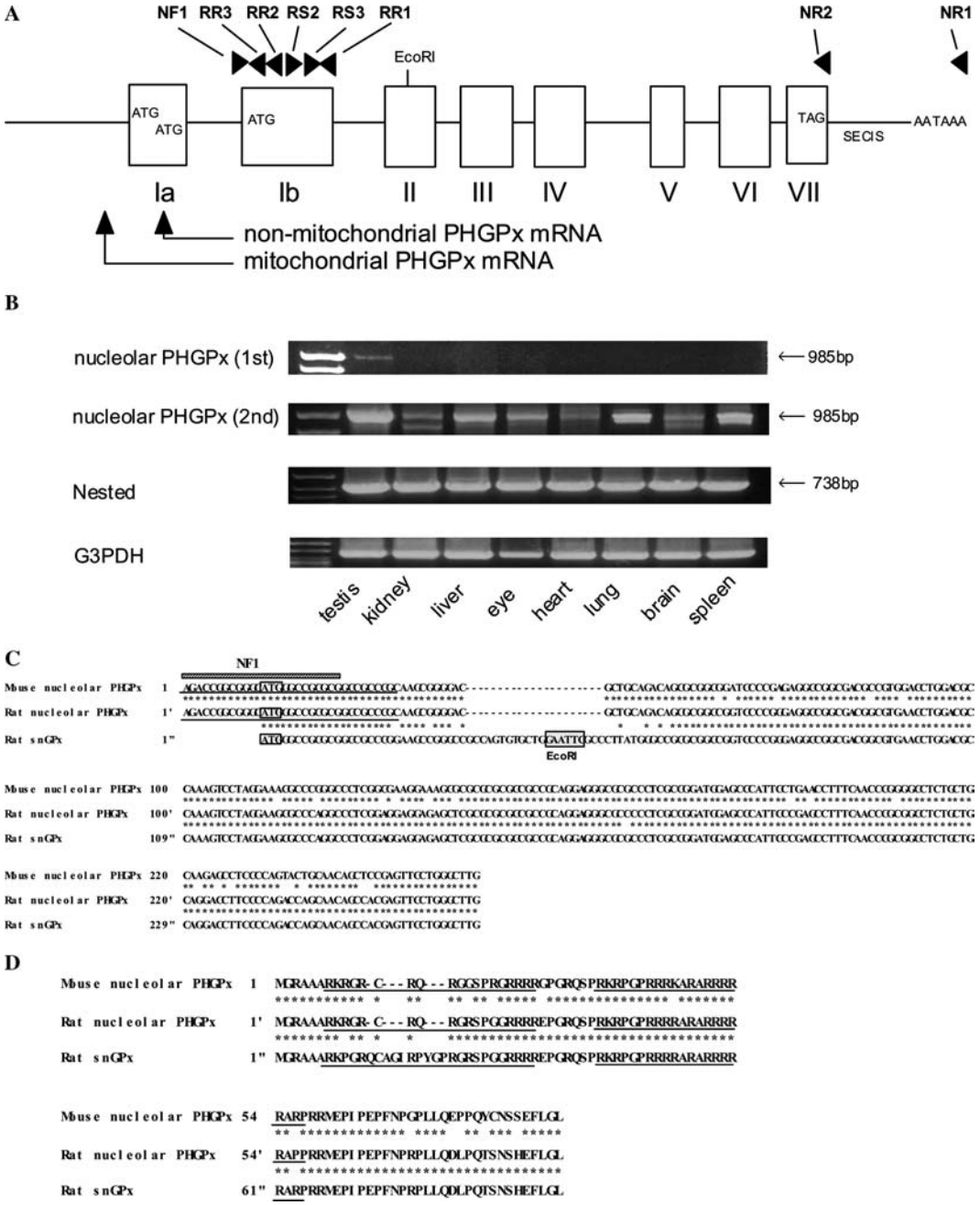

Fig. 1. Detection and cloning of mouse and rat nucleolar PHGPx. (A) The structure of the mouse PHGPx gene (Accession No. AB030643) and primers for the detection of nucleolar PHGPx. Arrowheads denoting NF1 and NR1 indicate the PCR primers used for detection of nucleolar PHGPx. Arrowheads denoting RS3 and NR2 indicate the PCR primers used for nested PCR. Arrowheads denoting RR3, RR2, RS2, RS3, and RR1 indicate the primers used for 5′-RACE methods. (B) Tissue distribution of nucleolar PHGPx mRNA. Only a 985 bp band is detected in rat testis by RT-PCR at first cycle using primer pairs NF1 and NR1. After cDNAs were extracted from sections around 985 bp in various tissues, the second PCR and nested PCR were performed from the cDNAs as a template using primer pairs NF1, NR1 and RS3, NR2. G3PDH was used as control. (C) Nucleotide sequences of exon Ib region in mouse (GenBank Accession No. AB072797) and rat nucleolar PHGPx (AB072798) and alignment of nucleolar PHGPx with rat sperm nuclei GPx (GenBank Accession No. AF274028). The open box and the shaded boxes indicate the initiation codon and *Eco*RI sites, respectively, in the exon Ib region. The shadow box indicates the sequence of the primer NF1. The underlines indicate the 5′-end sequences of rat and mouse identified by 5′-RACE method. The stars indicate the nucleic acid identical with that of rat nucleolar PHGPx. (D) The deduced amino acid sequence of exon Ib of nucleolar PHGPx and the alignment of nucleolar PHGPx with rat sperm nuclei GPx. The stars indicate the amino acid identical with that of rat nucleolar PHGPx. The nuclear targeting signals are indicated by a thin underline.

purified from rabbit serum through a peptide ligand affinity column. Immunohistochemical staining with anti-34 kDa nucleolar PHGPx pAb was performed as described previously [16]. In brief, 8 week mouse testes were fixed in 10% formalin and processed for embedding in paraffin wax. Immunohistochemical staining was performed with a combination of microwave-oven heating and the standard

streptavidin–biotin–peroxidase complex methods (LSAB kit; Dako, Copenagen, Denmark). The antibody used was anti-34 kDa nucleolar PHGPx pAb as described above. Staining of cytosol and nuclei was achieved with hematoxylin and eosin staining. To confirm the specificity of binding of pAb, normal rabbit serum, as negative control, was applied instead of a primary antibody. No staining was detected with the negative control.

Cell transfection and preparation of nuclear extract. A *Bam*HI fragment of pRNPHGPx1 constructed above was subcloned into SRα, as the expression vector [8], to construct pSRα-nucleolar PHGPx that encoded the nucleolar PHGPx. The expression vector SRα-nucleolar PHGPx and the control empty SRα vector were used for transient and stable transfections. For transient expression, L929 cells were seeded at 2×10^6 cells in 150-mm petri dishes 1 day before transfection. The cells were transfected with 10 μg pSRα-nucleolar PHGPx vector using 70 μl Lipofectamine reagents (Invitrogen) as described by the manufacturer's recommendation. For stable transfection, RBL-2H3 cells were transfected with pSRα-nucleolar PHGPx and pSV2neo by electroporation, as described previously [9]. Individual G418-resistant colonies were isolated with cloning cylinders. Levels of expression of PHGPx mRNA were determined by RT-PCR using LA*Taq* DNA polymerase with primer set, NF1 and NR1 as described above. Levels of expression of nucleolar PHGPx protein were determined by metabolic labeling with [^{75}Se]sodium selenite. Transfected L929 and RBL2H3 cells were labeled by addition to the culture medium of 0.14 μCi/ml [^{75}Se]sodium selenite (MURR, USA), as described previously, for 4 days. The nuclear and postnuclear fractions were then fractionated by a Nuclear Extract Kit (ACTIVE MOTIF). The purity of nuclear extracts was determined by immunoblot with anti-C23 nucleolus protein mAb. Nuclear fractions were lysed and immunoprecipitated with the anti-PHGPx mAb (3H10) and anti-cGPx pAb we made previously [16]. The immunoprecipitates and 50 μg of protein in the nuclear and postnuclear fractions were loaded and analyzed by 15% SDS–PAGE. Dried gels were scanned densitometrically with a Bio-imaging Analyzer (BAS2000; Fuji Film, Tokyo).

Cell viability. We used the previously established control line of cells (S1 cells) [8,9] and established nucleolar PHGPx overexpressing cell lines (N63, N120). S1, N63, and N120 were plated at 0.5×10^5 cells/well in flat-bottomed 96-well culture plates and cultured for 24 h. Individual transformants were exposed to indicated doses of actinomycin D and doxorubicin for 16 h. LDH release assay was used for the determination of cell viability, as described elsewhere [12]. In one series of experiments, cells were incubated for 24 h prior to exposure to actinomycin D and doxorubicin with 1 mM buthionine sulfoxamine (BSO) for depletion of intracellular glutathione (GSH).

Results and discussion

Cloning of full-length cDNA of nuclear types of PHGPx containing a novel signal sequence

To examine the cellular function of the nuclear types of PHGPx (sperm nuclei GPx, SnGPx), we first cloned full-length cDNA of nuclear types of PHGPx from mouse and rat testis by RT-PCR. For cloning of full-length cDNA of the nuclear type of PHGPx, we designed primers for nuclear type PHGPx from the sequence of mouse genomic DNA we previously cloned and sequenced as shown in Fig. 1A (Accession No. AB030643; [2]). The resulting 990 and 985 bp products of PCR for mouse and rat were amplified by RT-PCR with NF1 and NR1 primers, subcloned, and sequenced. We next determined the 5′-end sequence of mouse and rat nuclear PHGPx mRNA by the 5′-RACE method from rat and mouse testis with primers RS3, RR3, RR2, RS2, and phosphorylated RR1 primers. The 5′-ends of sequences identified by 5′-RACE method were coincided with the sequence of primer NF1 in Fig. 1C. The sequences and the deduced amino acid sequences in exon Ib of rat and mouse full-length nuclear types of PHGPx are indicated in Figs. 1C and D (Accession Nos. AB072798 and AB072797). The N-terminal amino acid of nuclear types of rat PHGPx we cloned in this study exhibited a nuclear signal sequence different from that reported previously for rat sperm nuclei GPx (SnGPx) (Accession No. AF274028; [5]), but identical to the exon Ib of rat gene identified recently (Accession No. RNO537598). The sequence and deduced amino acid of nuclear PHGPx of rat was highly homologous to that of nuclear PHGPx of mouse sequenced in this study. The sequence of the nuclear signal sequence of the N terminal of nuclear types of mouse PHGPx is the same as that of exon Ib in the genomic sequence of mouse we cloned previously [2]. The reported sequence-encoding rat SnGPx [5] has two *Eco*RI restriction sites; one exists in exon Ib, in Fig. 1C, and the other in exon II, in Fig. 1A. But the sequence of nuclear types of rat PHGPx we cloned has only one *Eco*RI site in exon II. We could not find two *Eco*RI sites; only the one *Eco*RI site in the 985 bp PCR products by analysis of the digestion of *Eco*RI (data not shown). We next examined the tissue distribution of nuclear types of rat PHGPx by RT-PCR. We could not detect the 985 bp band for the nuclear types of PHGPx except in the testis by the first RT-PCR (Fig. 1B). However, we found that the 985 bp band was amplified by the second PCR from cDNA extracted from gels around 985 bp in several tissues as shown in Fig. 1B. The bands amplified by the second PCR in several tissues were not artifacts, because 738 bp bands were also amplified by nested-PCR with RS3 and NR2 primers from cDNA extracted from gels around 985 bp (Fig. 1B). We also could not find two *Eco*RI sites; only the one *Eco*RI site in the 985 bp PCR products in several tissues by analysis of the digestion of *Eco*RI (data not shown). The sequences of PCR products amplified from liver and kidney of rat coincided with those of nuclear types of rat PHGPx we cloned, but not that of SnGPx. These results indicated that the nuclear types of rat PHGPx we cloned in the present study have clearly different sequences from that of the previously reported rat sperm nuclei GPx, and full lengths of the nuclear types of PHGPx mRNA were transcripted in several tissues.

Distribution of three types of PHGPx–YFP fusion proteins in HeLa cells

We found a novel sequence of nucleolar PHGPx in the biparticle nuclear targeting sequence in exon Ib, as

shown in Fig. 1D. We made the expression vectors for three types of PHGPx full-length–YFP fusion protein and YFP fused with rat exon Ib as shown in Fig. 2A to determine whether the three types of PHGPx could localize selectively at different organelle in living cells. Four expression vectors were transfected to HeLa and RBL2H3 cells by lipofectamine and the intracellular localization of fluorescence due to YFP was monitored with a confocal microscope (Figs. 2B–I). Two round specific regions with strong fluorescence were observed only in the nucleus of RBL2H3 and HeLa cells that expressed PHGPx–YFP fusion protein containing a rat novel sequence of exon Ib (Figs. 2C and F). The profile of fluorescence due to a novel nuclear type of PHGPx–YFP was identical to that of nucleolar specific protein C23 by immunostaining with anti-C23 mAb (Figs. 2D and E); [17]. This nucleolar localization of the nucleolar PHGPx–YFP fusion protein could also be observed in mouse L929 cells after transient expression (data not shown). The fluorescence due to PHGPx–YFP fusion protein with mouse exon Ib also was localized in nucleoli (data not shown). From these analyses, we named these nuclear types of PHGPx as nucleolar PHGPx. On the other hand, fluorescence of YFP fused with only a novel nuclear targeting sequence was also distributed within the whole nucleus (Fig. 2I). A previous report indicated that fluorescence of GFP fused with only the nuclear targeting sequence of SnGPx was distributed in the whole nucleus [5]. These results indicated that translocation of nucleolar PHGPx to nucleoli was required for both the nuclear targeting sequence in exon Ib and the internal amino acid sequence of PHGPx. On the other hand, discrete regions with strong fluorescence were observed in HeLa cells that expressed mitochondrial

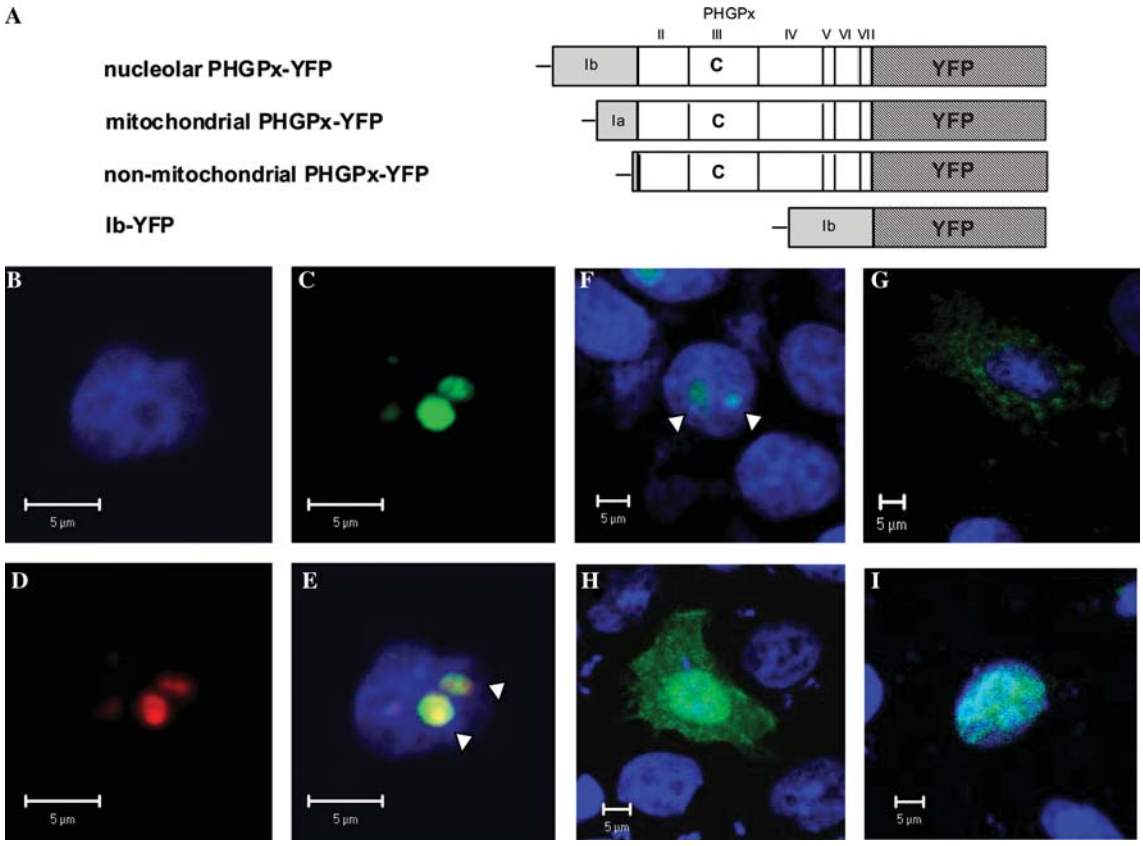

Fig. 2. Subcellular localization of three types of PHGPx–YFP (yellow fluorescent protein). (A) A schematic view of the structure of rat nucleolar, mitochondrial, non-mitochondrial PHGPx–YFP fusion protein, and YFP fused with only rat exon Ib. Nucleolar PHGPx–YFP contains exon Ib in the N terminus. Mitochondrial PHGPx–YFP contains full exon Ia in the N terminus. Non-mitochondrial PHGPx contains partial exon Ia in the N terminus. Ib–YFP contains only rat exon Ib in the N terminus. The C in exon III indicates that selenocysteine was converted to cysteine. (B–E) Nucleolar localization of nucleolar PHGPx–YFP in RBL2H3 cells. (B) Nuclear staining by Hoechst 33258 (C) Fluorescence of nucleolar PHGPx–YFP. (D) Immunostaining by Cy3 conjugated anti-nucleolar specific protein C23 mAb. (E) Merge. (F–H) Subcellular localization of YFP-tagged PHGPx in HeLa cells. (F) Nucleolar PHGPx–YFP, (G) mitochondrial PHGPx–YFP, (H) non-mitochondrial PHGPx–YFP, and (I) Ib–YFP. HeLa and RBL2H3 cells were transfected with 0.5 μg of fusion constructs using lipofectamine for 6 h. After 6 h cell culture, cells were stained with 1.6 μM Hoechst 33258 for 5 min. The nucleolar localization of nucleolar PHGPx–YFP fusion protein was confirmed by immunostaining with Cy3 conjugated anti-nucleolar specific protein C23 mAb. Fluorescence of YFP, Cy3, and Hoechst 33258 was observed using a confocal microscope LSM510 META. The green color shows the fluorescence of PHGPx–YFP fusion protein, blue color the nuclear staining by Hoechst 33258, and the red color the immunostaining by Cy3 conjugated anti-C23 mAb. Arrowheads indicate representative nucleoli. Scale bar, 5 μm.

PHGPx–YFP fusion protein (Fig. 2C). The profile of fluorescence due to mitochondrial PHGPx–YFP fusion protein was identical to that of mitochondrial cytochrome *c* oxidase subunit IV (data not shown). We previously indicated that exon Ia is a mitochondrial targeting signal, because fluorescence of GFP fused with only the mitochondrial targeting sequence was localized in mitochondria in HeLa and RBL2H3 cells [8,9]. By contrast, fluorescence was diffusely distributed in the nucleus and cytosol of cells having non-mitochondrial PHGPx–YFP fusion protein. These results indicated that the three types of PHGPx produced by alternative transcription from one gene were selectively distributed to the nucleolus, mitochondria, and within the whole cell including the nucleus.

Immunohistochemical analysis with anti-34 kDa nucleolar PHGPx in testis

We examined the expression of 34 kDa nucleolar PHGPx in testis of adult mouse using anti-34 kDa nucleolar PHGPx polyclonal antibodies. As shown in Fig. 3A, anti-nucleolar PHGPx pAb specifically detected a 34 kDa PHGPx in the nuclear extract of mouse testis, but not in the postnuclear fraction of mouse testis. Anti-nucleolar PHGPx pAb did not react with 20 kDa non-mitochondrial and mitochondrial PHGPx (Fig. 3A). This antibody recognized 34 kDa nucleolar PHGPx specifically in the nuclear extract of rat testis (data not shown). Immunohistochemical analysis with anti-nucleolar PHGPx pAb revealed that expression of nucleolar PHGPx was localized in the specific region within nucleus in spermatogonia, spermatocyte and spermatid (Figs. 3B and D). The profile of expression of nucleolar PHGPx by anti-nucleolar PHGPx was almost identical to that by anti-nucleolar specific protein C23 in spermatogonia, spermatocyte, and spermatid (Figs. 3C and D). These results indicated that the expression of nucleolar PHGPx was localized in nucleolus of spermatogonia and spermatocyte.

Expression of rat nucleolar PHGPx cDNA in mammalian cells

There are no reports of the expression of nucleolar PHGPx cDNA that includes the 3′-UTR in mammalian cells. We examined transient expression by transfection with rat nucleolar PHGPx expression vector into L929 cells using lipofectamine to determine whether cDNA for a rat nucleolar PHGPx that we cloned encoded

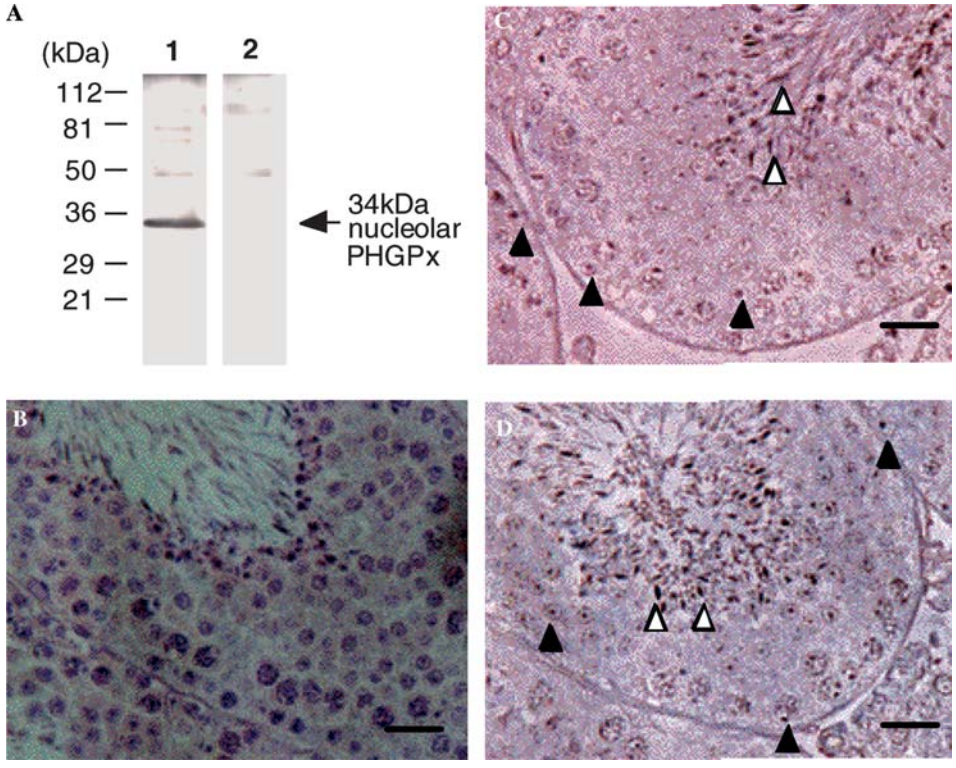

Fig. 3. Expression of 34 kDa nucleolar PHGPx in mouse testis. (A) Immunoblotting analysis with anti-34 kDa nucleolar PHGPx specific pAb of nuclear extract in mouse testis. Nuclear extract (1) and postnuclear fraction (2) in testis of adult mouse of eight week age. (B) Hematoxylin and eosin staining. (C,D) Immunohistochemical staining with anti-nucleolar specific protein C23.mAb (C) and anti-34 kDa nucleolar PHGPx specific pAb of adult mouse testis of 8 weeks of age. Scale bar, 100 μm. Black arrowhead indicate the spermatocyte and spermatogonia. White arrowhead indicate the spermatide.

34 kDa selenoprotein. Transfected L929 cells were grown in a medium containing [^{75}Se]sodium selenite for 4 days for determination of the intracellular distribution of nucleolar PHGPx. Figs. 4A and C show the subcellular distribution of ^{75}Se-labeled PHGPx and the other selenoproteins in L929 overexpressing nucleolar PHGPx. Nucleolar PHGPx of 34 kDa labeled with ^{75}Se were detected in the nuclear extract of L929 cells (Fig. 4A). No 34 kDa selenoprotein was detected in postnuclear fraction, which includes mitochondria, endoplasmic reticulum, and cytosol, although the other classes of ^{75}Se-labeled selenoproteins were detected in the postnuclear fraction (Fig. 4C). As shown in Fig. 4B, immunoprecipitation analysis with anti-PHGPx mAb showed that the 34 kDa selenoprotein expressed in the nuclear fraction of L929 cells was identical to nucleolar PHGPx and that large amounts of 20 kDa non-mitochondrial PHGPx were also detected in the nuclear fraction. Further, nucleolar specific C23 protein was detected in the nuclear fraction of L929 cells by immunoblot analysis (data not shown). These results indicated that cDNA for nucleolar PHGPx indeed encoded 34 kDa nucleolar PHGPx in mammalian cells.

We next isolated G418-resistant stable transfectants after RBL2H3 cells (rat basophile leukemia cells) had been transfected with the expression vector pSR-α-nucleolar PHGPx and pSV2neo by electroporation. RBL2H3 cells are suitable for the analysis of the intracellular role of PHGPx since the expression of PHGPx was very low [8]. We could not detect the 985 bp band for nucleolar PHGPx by the first RT-PCR in total RNA of RBL2H3 and S1 cells transfected by only empty pSR-α vector according to the method described in Fig. 1B. However, we could detect the 985 bp band for nucleolar PHGPx in N63 and N120 cell lines transfected with pSR-α-nucleolar PHGPx expression vector by the first RT-PCR (Fig. 4D). We determined the expression of nucleolar PHGPx in nuclear extracts of N63, N120, and control cell line S1 cells by metabolic labeling with [^{75}Se]sodium selenite (Fig. 4E). Selenoprotein of 34 kDa was detected in N63 and N120 cells, but not in S1 cells (Fig. 4E). On the

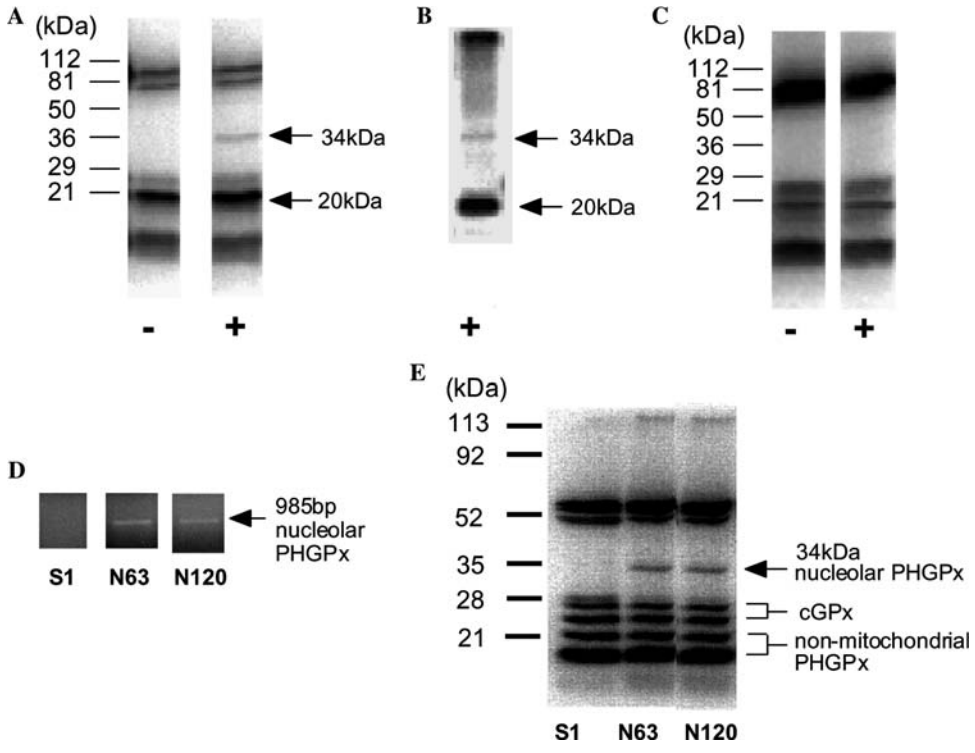

Fig. 4. Subcellular expression of nucleolar PHGPx in transfectants. (A–C) L929 cells were transfected transiently with SR-α expression vector including nucleolar PHGPx cDNA (+) or with SR- α vector without an insert (−). Transfected L929 cells were metabolically labeled with ^{75}Se (0.14 μCi) for 4 days. Then the nuclear fractions (A,B) and the postnuclear fraction (C) were fractionated by a Nuclear Extract Kit (ACTIVE MOTIF). Nuclear fractions were lysed and immunoprecipitated with anti-PHGPx mAb (3H10). The immunoprecipitates (B) and 50 μg of protein in the nuclear fraction (A) and the postnuclear fraction (C) were loaded and analyzed by 15% SDS–PAGE with subsequent autoradiography to detect the ^{75}Se-labeled proteins. (D,E) Expression of nucleolar PHGPx in established transfectants of RBL-2H3 cells. (D) Detection of mRNA for nucleolar PHGPx in stable transfectants (N63, N120) transfected with SR-α expression vector including nucleolar PHGPx cDNA and the control cell line (S1) transfected with only vector by RT-PCR. (E) Expression of ^{75}Se-labeled 34 kDa nucleolar PHGPx in nuclear fraction of stable transfectants (N63, N120) and the control cell line (S1). Transfected RBL2H3 cells were metabolically labeled with ^{75}Se (0.14 μCi) for 4 days. The nuclear fractions extracted by a Nuclear Extract Kit were loaded and analyzed by 15% SDS–PAGE with subsequent autoradiography to detect the ^{75}Se-labeled proteins. Arrows at 34 kDa indicate ^{75}Se-labeled nucleolar PHGPx and arrows at 20 kDa indicate ^{75}Se-labeled non-mitochondrial PHGPx.

other hand, 34 kDa selenoprotein was not detected in postnuclear fractions of S1, N63, and N120 cells (data not shown). We confirmed 34 kDa selenoprotein as nucleolar PHGPx, 20k- or 18k-Da selenoprotein as non-mitochondrial PHGPx by immunoprecipitation with anti-PHGPx mAb and 26- or 28-kDa selenoprotein as cGPx by immunoprecipitation with anti-cGPx pAb in the nuclear extract of S1, N63, and N120 cells (Fig. 4E). Levels of 34 kDa nucleolar PHGPx were significantly elevated in the nuclear extract of N63 and N120 cells as compared to S1 cells (Fig. 4E). No significant changes of the amounts of non-mitochondrial PHGPx and cGPx in nuclear extract were found by overexpression of nucleolar PHGPx in N63 and N120 cells (Fig. 4E). These results indicated that N63 and N120 cell lines were rat nucleolar PHGPx overexpressing cell lines.

Overexpression of nucleolar PHGPx suppresses cell death induced by actinomycin D and doxorubicin

Actinomycin D is an inhibitor of the RNA polymerase I that is localized in nucleolus [18]. Doxorubicin is an anticancer drug that inhibits topoisomerase II that exists in nucleolus [19,20]. Treatments of actinomycin D and doxorubicin induced the disruption of the structure of nucleolus [18,21]. We studied the effect of overexpression nucleolar PHGPx on the injury of cells from actinomycin D and doxorubicin. The viability of S1 cells decreased in a dose-dependent manner after treatment with actinomycin D and doxorubicin (Figs. 5A and B). By contrast, N63 and N120 cells that overexpressed nucleolar PHGPx showed resistance three to four times higher against the toxicity of actinomycin D and doxorubicin than did S1 cells (Figs. 5A

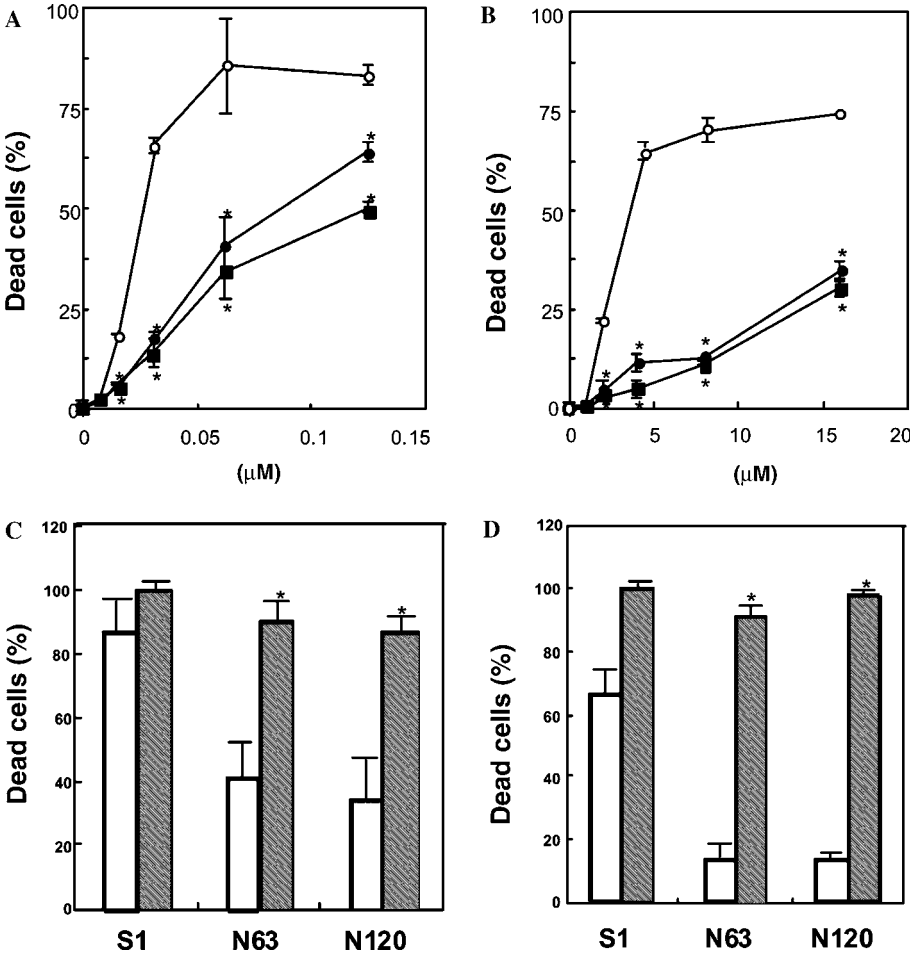

Fig. 5. Overexpression of nucleolar PHGPx suppressed cell death induced by actinomycin D and doxorubicin. (A,B) Control cells (S1 cells; open circles) and cells that overexpressed nucleolar PHGPx (N63 cells; closed circles, and N120 cells; closed squares) were placed at 0.5×10^5 cells/well in DMEM plus 5% FCS. Cells were also exposed to the indicated doses of actinomycin D (A) and doxorubicin (B) for 16 h. Data are means ± SD of results from three replicates in each case. $*p < 0.05$, by comparison to S1 cells. (C,D) Effects of buthionine sulfoximine (BSO) on the resistance to actinomycin D and doxorubicin-induced cell death. Individual cultures were treated for 24 h with 1 mM BSO (shadow bars) or not (open bars) to deplete cells of intracellular GSH and then exposed to 0.07 μM actinomycin D (C) and 8 μg/ml doxorubicin (D) for 16 h. Cell viability was estimated from the release of LDH as described in Materials and methods. Data are means ± SD of results from three replicates in each case. $*p < 0.05$, by comparison to non-BSO treated cells.

and B). The effects of actinomycin D and doxorubicin on the viability of S1, N63, and N120 cells, which had been depleted of GSH, were examined to estimate whether or not the resistance to actinomycin D and doxorubicin in N63 and N120 cells resulted from overexpression of nucleolar PHGPx. Buthionine sulfoximine (BSO), an inhibitor of the synthesis of glutathione, inhibits the activity of glutathione-dependent peroxidases, such as cGPx and PHGPx, by lowering the level of glutathione in cells. When N63 and N120 cells pretreated with BSO for 24 h were exposed to actinomycin D and doxorubicin, the cells lost their resistance to the toxicity of actinomycin D and doxorubicin (Figs. 5C and D). These results confirm that resistance of N63 and N120 cells to actinomycin D and doxorubicin toxicity is due to the overexpression of nucleolar PHGPx in nucleoli.

The nucleolus is a subnuclear organelle containing the ribosomal RNA gene clusters and ribosome biogenesis factors [22]. Recent studies suggest it may also have roles in RNA transport, RNA modification, cell cycle regulation, and aging [23]. However, little has been published on the role of nucleoli in cell death. In this study, overexpression of nucleolar PHGPx suppressed cell death induced by actinomycin D and doxorubicin that induce damage in nucleoli. However, overexpression of nucleolar PHGPx in N63 and N120 cell lines could not suppress the cell death caused by 2-deoxyglucose and staurosporine that induced the release of the cytochrome *c* from mitochondria and apoptosis (data not shown). We previously reported that overexpression of mitochondrial PHGPx, but not non-mitochondrial PHGPx, could suppress the cell death induced by 2-deoxyglucose and staurosporine [12]. These results suggested that each PHGPx localized in individual organelle played a role to protect different death pathways. The full details of the mechanism of resistance to actinomycin D and doxorubicin by nucleolar PHGPx remain to be clarified. However, production of reactive oxygen species (ROS) is also thought to have the cytotoxic effect of doxorubicin and actinomycin D on cancer cells [24,25]. PHGPx has been shown to reduce lipid hydroperoxide, DNA hydroperoxide, and hydrogen peroxide [1,26]. The activity of glutathione-dependent PHGPx might be expressed in nucleoli since glutathione and glutathione reductase are present in nucleoli [27,28]. The evidence here suggests that nucleolar PHGPx plays a novel, and important, role in protecting the nucleolus from damage by oxidative stress; and the protection of the nucleolus from damage is an important factor in the regulation of cell death.

Acknowledgments

We thank Ms. Ayumi Wada and Mr. Noritake Okamura for their expert technical assistance. This work was supported in part by Grant-in-Aid 15790045 from the Ministry of Education, Science and Culture of Japan by a Kitasato University Research Grant for Young Researchers, and by the foundation from the Association for the Progress of New Chemistry.

References

[1] H. Imai, Y. Nakagawa, Biological significance of phospholipid hydroperoxide glutathione peroxidase (PHGPx, GPx4) in mammalian cells, Free Radic. Biol. Med. 34 (2) (2003) 145–169.
[2] H. Imai, F. Hirao, T. Sakamoto, K. Sekine, Y. Mizukura, M. Saito, T. Kitamoto, M. Hayasaka, K. Hanaoka, Y. Nakagawa, Early embryonic lethality caused by targeted disruption of the mouse PHGPx gene, Biochem. Biophys. Res. Commun. 305 (2) (2003) 278–286.
[3] M. Arai, H. Imai, D. Sumi, T. Imanaka, T. Takano, N. Chiba, Y. Nakagawa, Import into mitochondria of phospholipid hydroperoxide glutathione peroxidase requires a leader sequence, Biochem. Biophys. Res. Commun. 227 (2) (1996) 433–439.
[4] H. Kuhn, A. Borchert, Regulation of enzymatic lipid peroxidation: the interplay of peroxidizing and peroxide reducing enzymes, Free Radic. Biol. Med. 33 (2) (2002) 154–172.
[5] H. Pfeifer, M. Conrad, D. Roethlein, A. Kyriakopoulos, M. Brielmeier, G.W. Bornkamm, D. Behne, Identification of a specific sperm nuclei selenoenzyme necessary for protamine thiol cross-linking during sperm maturation, FASEB J. 15 (7) (2001) 1236–1238.
[6] R. Puglisi, F. Tramer, E. Panfili, F. Micali, G. Sandri, C. Boitani, Differential splicing of the phospholipid hydroperoxide glutathione peroxidase gene in diploid and haploid male germ cells in the rat, Biol. Reprod. 68 (2) (2003) 405–411.
[7] H. Imai, D. Sumi, A. Hanamoto, M. Arai, A. Sugiyama, Y. Kucino, Y. Nakagawa, Molecular cloning and functional expression of a cDNA for rat phospholipid hydroperoxide glutathione peroxidase: 3′-untranslated region of the gene is necessary for functional expression, J. Biochem. (Tokyo) 118 (5) (1995) 1061–1067.
[8] H. Imai, D. Sumi, H. Sakamoto, A. Hanamoto, M. Arai, N. Chiba, Y. Nakagawa, Overexpression of phospholipid hydroperoxide glutathione peroxidase suppressed cell death due to oxidative damage in rat basophile leukemia cells (RBL-2H3), Biochem. Biophys. Res. Commun. 222 (2) (1996) 432–438.
[9] M. Arai, H. Imai, T. Koumura, M. Yoshida, K. Emoto, M. Umeda, N. Chiba, Y. Nakagawa, Mitochondrial phospholipid hydroperoxide glutathione peroxidase plays a major role in preventing oxidative injury to cells, J. Biol. Chem. 274 (8) (1999) 4924–4933.
[10] H. Imai, K. Narashima, M. Arai, H. Sakamoto, N. Chiba, Y. Nakagawa, Suppression of leukotriene formation in RBL-2H3 cells that overexpressed phospholipid hydroperoxide glutathione peroxidase, J. Biol. Chem. 273 (4) (1998) 1990–1997.
[11] H. Sakamoto, H. Imai, Y. Nakagawa, Involvement of phospholipid hydroperoxide glutathione peroxidase in the modulation of prostaglandin D2 synthesis, J. Biol. Chem. 275 (51) (2000) 40028–40035.
[12] K. Nomura, H. Imai, T. Koumura, M. Arai, Y. Nakagawa, Mitochondrial phospholipid hydroperoxide glutathione peroxidase suppresses apoptosis mediated by a mitochondrial death pathway, J. Biol. Chem. 274 (41) (1999) 29294–29302.
[13] H. Sakamoto, T. Tosaki, Y. Nakagawa, Overexpression of phospholipid hydroperoxide glutathione peroxidase modulates acetyl-CoA, 1-*O*-alkyl-2-lyso-*sn*-glycero-3-phosphocholine acetyltransferase activity, J. Biol. Chem. 277 (52) (2002) 50431–50438.
[14] K. Nomura, H. Imai, T. Koumura, T. Kobayashi, Y. Nakagawa, Mitochondrial phospholipid hydroperoxide glutathione peroxidase inhibits the release of cytochrome *c* from mitochondria by suppressing the peroxidation of cardiolipin in hypoglycaemia-induced apoptosis, Biochem. J. 351 (Pt 1) (2000) 183–193.

[15] H. Imai, T. Koumura, R. Nakajima, K. Nomura, Y. Nakagawa, Protection from inactivation of the adenine nucleotide translocator during hypoglycaemia-induced apoptosis by mitochondrial phospholipid hydroperoxide glutathione peroxidase, Biochem. J. 371 (Pt 3) (2003) 799–809.
[16] H. Imai, K. Suzuki, K. Ishizaka, S. Ichinose, H. Oshima, I. Okayasu, K. Emoto, M. Umeda, Y. Nakagawa, Failure of the expression of phospholipid hydroperoxide glutathione peroxidase in the spermatozoa of human infertile males, Biol. Reprod. 64 (2) (2001) 674–683.
[17] Y.P. Li, R.K. Busch, B.C. Valdez, H. Busch, C23 interacts with B23, a putative nucleolar-localization-signal-binding protein, Eur. J. Biochem. 237 (1) (1996) 153–158.
[18] C. Verheggen, G. Almouzni, D. Hernandez-Verdun, The ribosomal RNA processing machinery is recruited to the nucleolar domain before RNA polymerase I during *Xenopus laevis* development, J. Cell Biol. 149 (2) (2000) 293–306.
[19] S. Goto, Y. Ihara, Y. Urata, S. Izumi, K. Abe, T. Koji, T. Kondo, Doxorubicin-induced DNA intercalation and scavenging by nuclear glutathione *S*-transferase pi, FASEB J. 15 (14) (2001) 2702–2714.
[20] J.S. Andersen, C.E. Lyon, A.H. Fox, A.K. Leung, Y.W. Lam, H. Steen, M. Mann, A.I. Lamond, Directed proteomic analysis of the human nucleolus, Curr. Biol. 12 (1) (2002) 1–11.
[21] P.K. Chan, M.B. Aldrich, B.Y. Yung, Nucleolar protein B23 translocation after doxorubicin treatment in murine tumor cells, Cancer Res. 47 (14) (1987) 3798–3801.
[22] M. Srivastava, H.B. Pollard, Molecular dissection of nucleolin's role in growth and cell proliferation: new insights, FASEB J. (14) (1999) 1911–1922.
[23] M.O. Olson, K. Hingorani, A. Szebeni, Conventional and nonconventional roles of the nucleolus, Int. Rev. Cytol. 219 (2002) 199–266.
[24] B.K. Sinha, E.G. Mimnaugh, Free radicals and anticancer drug resistance: oxygen free radicals in the mechanisms of drug cytotoxicity and resistance by certain tumors, Free Radic. Biol. Med. 8 (6) (1990) 567–581.
[25] K. Kajiwara, K. Ikeda, R. Kuroi, R. Hashimoto, S. Tokumaru, S. Kojjo, Hydrogen peroxide and hydroxyl radical involvement in the activation of caspase-3 in chemically induced apoptosis of HL-60 cells, Cell. Mol. Life Sci. 58 (3) (2001) 485–491.
[26] Y. Bao, P. Jemth, B. Mannervik, G. Williamson, Reduction of thymine hydroperoxide by phospholipid hydroperoxide glutathione peroxidase and glutathione transferases, FEBS Lett. 410 (2–3) (1997) 210–212.
[27] S. Soboll, S. Grundel, J. Harris, V. Kolb-Bachofen, B. Ketterer, H. Sies, The content of glutathione and glutathione *S*-transferases and the glutathione peroxidase activity in rat liver nuclei determined by a non-aqueous technique of cell fractionation, Biochem. J. 311 (Pt 3) (1995) 889–894.
[28] L.K. Rogers, S. Gupta, S.E. Welty, T.N. Hansen, C.V. Smith, Nuclear and nucleolar glutathione reductase, peroxidase, and transferase activities in livers of male and female Fischer-344 rats, Toxicol. Sci. 69 (1) (2002) 279–285.